Desalination and Water Treatment
www.deswater.com

doi: 10.5004/dwt.2021.27298

227 (2021) 58–67
July

Textile water treatment via adsorption of basic brown 1 dye on ZnO/PVC nanocomposite membrane through membrane adsorption process

Sanaa Naeim[a], Abeer A. Emam[a], Mahmoud F. Mubarak[b,*], R. Hosny[c,*]

[a]*FFaculty of Science, El-Azhar University, Cairo, Egypt*
[b]*Petroleum Application Department, Egyptian Petroleum Research Institute (EPRI), 1 Ahmed El-Zomor, Box No. 11727, Nasr City, Cairo, Egypt, Tel. +(202)22747847*
[c]*Production Department, Egyptian Petroleum Research Institute (EPRI), 1 Ahmed El-Zomor, Box No. 11727, Nasr City, Cairo, Egypt, Tel. +(202)22747847; Fax: +(202)22747433; emails: fathy8753@yahoo.com (M.F. Mubarak), dr.rashahosny@yahoo.com (R. Hosny)*

ABSTRACT

In this paper, PVC/ZnO nanocomposite membrane was prepared to remove toxic textile dye (basic brown 1) from synthetic wastewater solutions. Fourier transform infrared, scanning electron microscopy, X-ray diffraction, transmission electron microscopy, and zeta potential (ZP) investigated the prepared nanocomposite membrane. The results showed zinc present in the membrane as nanoparticle needles with the asymmetric spread in them. The hydrophilic behavior of the membrane surface was due to zinc oxide, which exhibits significant efficiency for the removal of commonly used basic brown 1 dye from an aqueous system. The prepared nanocomposite membrane efficiency was investigated by different parameters like pH, dye concentration, PVC/ZnO ratio, and time. The kinetics and isotherm of adsorption basic brown 1 dye adsorbed on PVC/ZnO nanocomposite membrane were studied. The efficiency of the prepared membrane reached 98.6% for dye removal from synthetic water after 60 min. The results showed that the pseudo-second-order model was favorable for the adsorption kinetics and isotherm. This assumes that the adsorption mechanism is the chemical adsorption process. It also showed that the Langmuir isothermal model is appropriate for the adsorption process, which means the adsorption was taking place as a monolayer process on homogeneous sites. Finally, the results revealed that the prepared nanocomposite membrane was less expensive, improving performance, and extending life expectancy. The separation process with low energy requirements, including low ultra-filtration and adsorption and mobility, was characterized by the extremely rapid reaction and high selectivity to remove the basic brown 1 dye.

Keywords: Ultrafiltration adsorption; Basic brown 1 dye rejection; Textile wastewater treatment; PVC/ZnO nanocomposite membrane

1. Introduction

The dyeing and printing industries use a huge amount of water in their manufacturing processes [1]. The wastewater from the dyeing and printing industries is identified as the most polluted water considering the volume generate as well as the effluent composition [2]. In the textile industry, 2,000,000 REF tons of dyes are turned to effluent every year during dyeing, finishing, and printing operations due to the dyeing process inefficiency [3]. The increased demand of dyed product which is dyed by synthetic dyes produce wastewater after dyeing. This wastewater is the main source of the pollution problem in recent time. Because most of the industry uses conventional wastewater treatment plants, some of the effects of dye-bearing wastewater are aesthetic pollution of the environment and also carcinogenicity due to their degradation products [4]. When flowing into the river surfaces, pollutants in wastewater create adverse effects on the ecosystem and human health, which is irreversible in some cases [5–10]. Water recycling will be important in the future, an essential part of incoming freshwater [11]. This recycling includes improving wastewater quality and freshwater use standards [12–14].

Wastewater treatment in the textile industry aims to reduce the color and presence of dissolved organic molecules. The current treatment view is focused on the reuse

* Corresponding authors.

of wastewater as a source, not waste [15,16]. Conventional methods are insufficient to attain the desired water quality as the current wastewater treatment methods depend mainly on biochemical decomposition [17–20]. Consider incorporating water reuse will lower the water quality and increase secondary water sources [21,22].

Moreover, the percentage of water reused is limited, with large waste losses [23]. Various physical, chemical, and biological techniques have been developed to remove dyes from polluted water [24]. Many techniques like electrochemical coagulation, reverse osmosis, nanofiltration, ultrafiltration using membrane technique, adsorption on activated materials, etc., are used for the dye removal from wastewater. Membrane filtration has been found to be an efficient and economical process for the treatment of dyeing industry effluent [25–31]. Polyvinyl chloride (PVC) is a versatile thermoplastic widely used globally, with demand exceeding 35 million tons per year [30]. Polyvinyl chloride (PVC) was characterized by high chemical stability and high physical strength to withstand high pressures during the desalination or water treatment process. Zinc oxide nanoparticles (ZnO NPs) are of a high adsorption capacity of dyes and decomposition of dyes due to their positive charge that increasing the chemical adsorption strength through the formation of coordinating bond between the positive surface and the lone pair of electrons of dye nitrogen atoms [31–37].

In this paper, the new nanocomposite membrane, which was prepared for water treatment from dye, is based on physical separation without adding chemicals in the feed stream and without changing the phase. Moreover, it can be operated without heating. Therefore, this separation process is usually less energetic than traditional separation techniques (distillation, crystallization, and adsorption). Also, the membrane is less expensive, improving performance, and extending life expectancy. This study will investigate the applicability of the ZnO/PVC in the adsorption-ultrafiltration process for toxic dye removal, that is, basic brown 1 dye from synthetic wastewater solutions. The main parameters, such as pollutants, pH, and PVC/ZnO ratios, have been determined for the dyes' removal performance. Also, retentate and permeate parameters have been calculated.

2. Experimental

2.1. Chemicals

Polyvinyl chloride (Mw PVC = 58,000 Da) was used for membrane preparation from Merck (Germany), $(Zn(CH_3COO)_2{\cdot}2H_2O) \geq 99\%$ purity, NH_4OH. The other chemicals were used without further purification. Basic brown 1 dye has been purchased from Sisco Research Laboratories Pvt., Ltd., Maharashtra, India (Fig. 1). NaOH, (Sigma-Aldrich) product in China, and H_2SO_4 (98%) have been produced from S. D. Fine Chemicals Ltd., Mumbai, India, were used for adjusting the pH during the measurements of zeta potential. Distilled water, DI water, DMF solution, and ethanol.

2.2. Synthesis of ZnO nanoparticles

By using the sol–gel method, zinc oxide nanoparticles (ZnO NPs) were synthesized. In order to prepare a sol, 3.33 g of zinc acetate dihydrate $(Zn(CH_3COO)_2{\cdot}2H_2O) \geq 99\%$ purity and 13.3 g of sodium hydroxide (NaOH) ≥ 98% were weighted using a weighing balance. After that, 3.33 g of zinc acetate dihydrate was dissolved with 25 mL of distilled water, and 13.3 g of NaOH was dissolved in 16.6 mL of distilled water; then stirred the solutions with a fixed rate for about 5 min. After mixed well, the NaOH solution was poured into the above solution with stirring for 5 min. Then, titrate ethanol to the previous solution, a white ppt was formed after the reaction (endpoint) [32].

2.3. Membrane fabrication

PVC (blank sample) and ZnO NPs were prepared separately then mixed to prepare PVC/ZnO nanocomposite membranes. Firstly, a solution of 15% PVC (wt/v) DMF was prepared. Afterward, the weight of a certain ZnO powder was added to the above-prepared solution at room temperature for 40 h with stirring (150 rpm) to get a 1, 3, 5 wt.% ZnO soln. The solutions of PVC, ZnO were heated at temperature 70°C by oil bath for 24 h with fixed stirring (150 rpm) to get the solution homogeneously. Leave the ZnO and PVC solutions for 24 h, then mixed them at (50°C (oil bath), 1 h, and 250 rpm). After that, leave them without stirring (48 h and 50°C) to sufficient air bubbles release. After that, these solutions were poured onto glass plates using a 250 μm thick film applicator, and left to dry at room temperature overnight to get the membrane film. The dried membrane film was immersed in distilled hot water for a time to remove the solvent and coagulate the polymer, so we get a thin film membrane separated from the glass plate. The prepared membrane was washed with hot water and dried in the air at room temperature for 24 h.

2.4. Membrane filtration and adsorption

Typical adsorption and ultrafiltration used for the removal of basic brown 1 dye are shown in Fig. 2. It consists

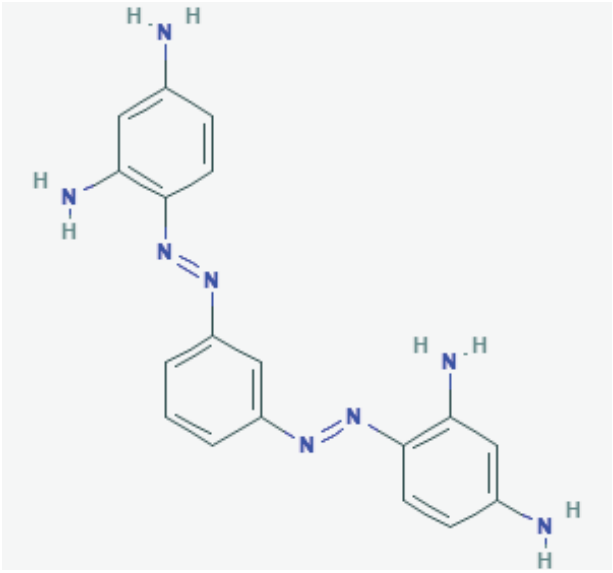

Fig. 1. Chemical structure of basic brown 1 dye.

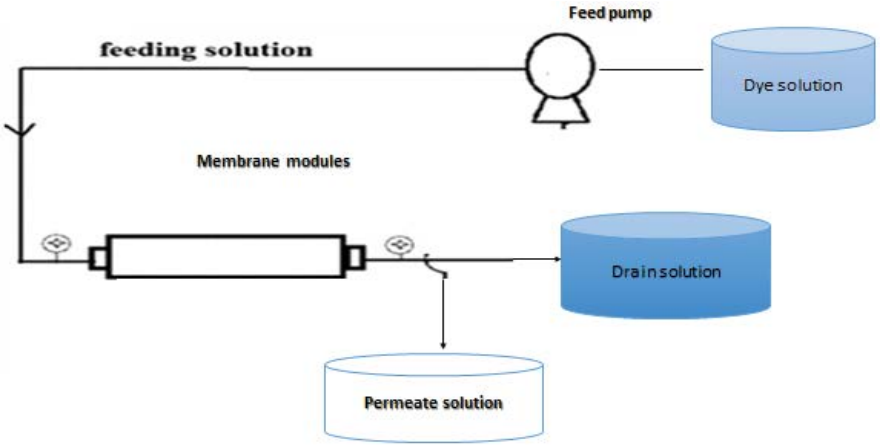

Fig. 2. Typical experimental setup of the membrane system.

of a 5 L filtration system tank. The membrane filtration has an outer jacket to preserve the temperature filtration system constant. A centrifugal pump of 0.87 HP power rating is connected to the bottom side of the membrane filtration system to draw the dye solution and sent to the PVC/ZnO nanocomposite membrane. The prepared nanocomposite membrane modules were used in the experiments applied as a thin film plate in the system. Control valves, pressure gauges, and rotameter have been placed inline between the filtration system and PVC/ZnO nanocomposite membrane to maintain the desired flow rates and pressures. The preparation and use of the composite membrane material in the hybrid system were given below.

Weigh a suitable quantity of ZnO NPs and added to the basic brown 1 dye solution in a separate container. All of the solutions have been transferred to the composite membrane filtration system after vigorous mixing. A typical experimental setup of the membrane system is shown in Fig. 2. The ZnO NPs used in this study have been attached to the surface membrane, not a suspended state in the dye solution. During the experimental processes, the dye solution was passed through the ultrafiltration membrane and recycled back to the membrane filtration system. All systems were worked in a closed-loop.

After removing the dye and filtering the membrane at a certain pressure and specific flow rate, we notice that the treated water comes out from the membrane as effluent or permeate, which is examined by a spectrophotometer at a wavelength of 590–630 nm.

2.5. Characterization and analysis

Fourier transform infrared (FTIR) analysis was investigated the binding properties of PVC, PVC/ZnO nanocomposite membranes via range spectral of 3,500–500 cm^{-1} with 4 cm^{-1} resolution by Perkin Elmer spectrum 1000 spectrum (Germany). Properly washed and dried samples of synthesized PVC, PVC/ZnO nanocomposite membranes were used for X-ray diffraction (XRD) analysis using Ultima IV (Rigaku, Japan) at the wavelength of 1.5406 Å. Scanning electron microscopy (SEM) was examined the morphology of PVC/ZnO nanocomposite membrane by (SU3500, Hitachi (Germany) with spectral imaging system Thermo Scientific (Germany) NSS (energy-dispersive X-ray spectroscopy), the tape of a detector (BSE-3D), acceleration voltage (15.0 kV), the working distance (11.6 mm), pressure (in the case of variable vacuum conditions) (40 Pa). Transmission electron microscopy (TEM) analysis used for enlarged ZnO NPs, thus promoting nanoparticles linked rough nanowire-like structure. Zeta potential AsurPASSelectrokinetic analyzer (Anton-Paar GmbH, Graz, Austria) has been used to measure the zeta potential (ZP) on the surfaces of the membrane. The potential measurements of all membranes were performed in 1 mM KCl of background electrolyte solution using the Fairbrother–Mastin method. The pH values for all measurements were estimated by using HCl and NaOH solutions.

2.6. Adsorption kinetics

Adsorption kinetics were studied using pseudo-first and pseudo-second-order kinetics models of the basic brown dye 1 adsorbed on a PVC/ZnO nanocomposite membrane to postulate the adsorption mechanism. These models have been widely used to describe the kinetics of adsorption [38].

The pseudo-first-order kinetic model rate equation is given by Eq. (1):

$$\log\left(q_e - q_t\right) = \log q_e - \frac{k_1}{2.303}t \tag{1}$$

The pseudo-second-order rate equation is given by Eq. (2):

$$\frac{q_t}{t} = \frac{1}{k_2 q_e^2} + \frac{q_e}{t} \tag{2}$$

where q_t and q_e are the amounts of adsorbed metal ions (mg/g) at equilibrium and time t (min); k_1 is the Lagergren rate constant of the pseudo-first-order adsorption (min^{-1}); k_2 is the rate constant of pseudo-second-order (g mg^{-1} min^{-1})

To calculate the constant rate values (k_1), the linear curve of $\log(q_e - q_t)$ vs. time (min) were plotting, while (q_e/t) vs. time (min) was used to calculate the constant rate values (k_2).

2.7. Adsorption isotherm

Models of Langmuir and Freundlich are two popular isotherm adsorption models that are applied to determine the affinity of sorbent and adsorbate and to explain the adsorption mechanism [39]. In the Langmuir model, the adsorption was taking place on homogeneous sites as a monolayer process, while in the Freundlich model, the adsorption was a multilayer process and heterogeneous adsorption surface. Langmuir model equation is given by Eq. (3) as follows:

$$\frac{C_e}{q_e} = \frac{1}{K_l q_m} + \frac{C_e}{q_m} \tag{3}$$

where q_e is the adsorption capacity at equilibrium (mg/g); q_m is the maximum adsorption capacity (mg/g); C_e is the concentration of metal ions after adsorption (mg/l); K_L is the affinity constant (L/g).

Calculate the values of K_L and q_m by plotting the curve C_e/q_e vs. C_e. Separation factor (R_L) was calculated from Eq. (4):

$$R_L = \frac{1}{\left(1 + C_0 K_l\right)\pi r^2} \tag{4}$$

where C_0 is the initial concentration of dye; K_l is the Langmuir constant.

The separation factor (R_L) was determined to determine whether the adsorption is favorable or unfavorable. A favorable adsorption when $0 < R_L < 1$, while unfavorable adsorption in $R_L > 1$, the adsorption process is linear adsorption $R_L = 1$, and irreversible adsorption represents in $R_L = 0$.

The Freundlich model is represented by Eq. (5):

$$\log q_e = \log K_f + \frac{1}{n}\log C_e \tag{5}$$

where q_e is the adsorption capacity at equilibrium(mg/g); C_e is the concentration of dye after adsorption (mg/L); K_f is the Freundlich isotherm constant (L/g); n is the heterogeneity factor (index of the diversity).

By plotting the curve $\log q_e$ vs. $\log C_e$, the Freundlich constants can be obtained. The exponent (n) is an index of the diversity of free energies associated with the adsorption of the solute by multiple components of a heterogeneous adsorbent. The isotherm is linear when $n = 1$, while the isotherm is concave and adsorbate is bound with weaker and weaker free energies when $n < 1$, and $n > 1$, the isotherm is convex. More adsorbate existence on the adsorbent improves the free energies of extra adsorption.

3. Results and discussion

3.1. Prepared nanocomposite membrane characterizations

3.1.1. Fourier transform infrared

FTIR was used to confirm the constituents of the synthesized PVC, PVC/ZnO nanocomposite membranes Fig. 3. From the FTIR results, the PVC/ZnO nanocomposite membrane was showed a similar pattern of spectra confirming the fingerprint of PVC. Group –CH appears at 1,259 cm^{-1}, beak at 1,430 cm^{-1} for $–CH_2$ related to symmetric bending. The –OH group has a stretching beak at 3,000 cm^{-1} that is related to ZnO. This signified that only PVC existed in the nanocomposite membrane. The slight shift of the peaks after blending with ZnO indicated that there was an interaction between the polymer and ZnO nanoparticles. The O–H group has a broad beak at 3,438 cm^{-1} that indicated the presence of an H-bond with water molecules [27]. –C=C alkene stretching has bands at 2,926 and 2,235 cm^{-1}. Meanwhile, the C–O having a beak at 1,620 cm^{-1} indicate the surface of the OH group.

3.1.2. XRD analysis

XRD analysis was carried out to study the crystallinity nature of the PVC and PVC/ZnO nanocomposite membranes Fig. 4. It was well-known that the PVC exhibit a semi-crystalline shape at 2θ of 20° and 40°. A large peak of 20° at 2θ for the ZnO NPs was found. While the PVC fillers were added, the peak intensities of the PVC/ZnO nanocomposite membrane were decreased. This reveals that the addition of PVC fillers to the ZnO NPs matrix greatly increased the domain of the amorphous region (for example, the intensity of the XRD crystal peak decreased). Particle size and crystal lattice obtained from XRD of prepared ZnO nanoparticle. The peaks that attributed to the hexagonal phase of PVC were 31.79°, 34.46°, 36.25°, 47.47°, 56.61°, 62.87°, 66.43°, 68.07°, and 69.18° corresponding to lattice planes (1 0 0), (0 0 2), (1 0 1), (1 0 2), (1 1 0), (1 0 3), (2 0 0), (1 1 2), and (2 0 1), respectively.

3.1.3. SEM image

The surface structures of the fabricated PVC/ZnO nanocomposite membranes for basic brown 1 dye removal are

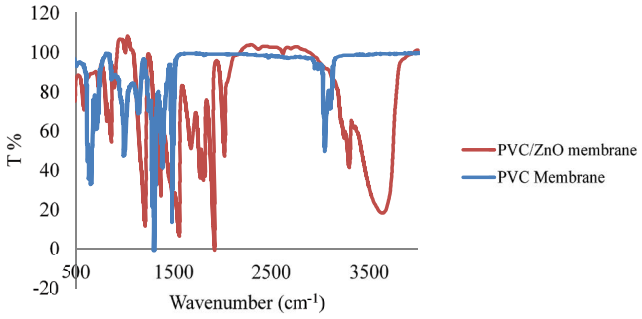

Fig. 3. FTIR spectrum of the synthesized PVC/ZnO, PVC nanocomposite membranes.

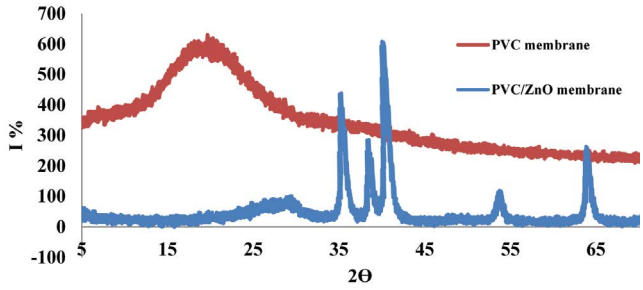

Fig. 4. XRD spectra for the synthesized PVC and PVC/ZnO nanocomposite membranes.

displayed in Fig. 5. The PVC membrane prepared from PVC waste is characterized by the presence of a thick and dense surface, which increases the presence of mesoporous and microporous (nanoscale range). The SEM image in Fig. 5 indicated the pore size charge from the ultrafiltration to NF range where it is from 1–10 nm, also the distribution very smooth within a rough surface, so we get a high rejection and good flux. We can see from the 56 μ image that ZnO NPs have a spherical shape with regular aggregates and accumulation on the membrane surface.

3.1.4. HR-TEM analysis

Regarding the morphological characterization, Fig. 6 shows high-resolution TEM images of ZnO NPs obtained by the chemical precipitation method at a calcination temperature of 500°C. Although some polyhedron morphology could be observed, the micrograph showed almost spherical nanoparticles as the predominant particles. As shown in Fig. 6, the particles tend to agglomerate. These agglomerations may occur during the calcination process due to the high surface energy of the nanoparticles. Particle size was in the range ~18 nm calculated from the analysis of TEM images, which is in good agreement with the results obtained from the XRD pattern.

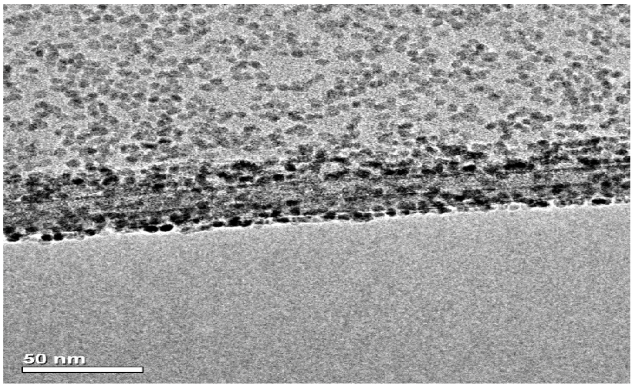

Fig. 5. SEM images of the synthesized PVC/ZnO nanocomposite membrane.

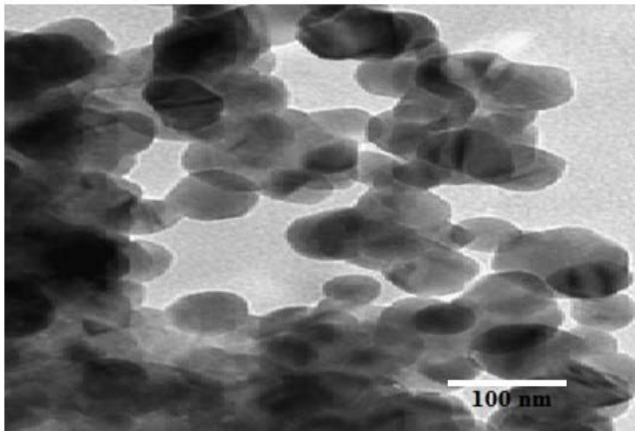

Fig. 6. HR-TEM images of the investigated ZnO NPs powder were obtained at 500°C for 2 h.

3.1.5. Zeta potential of PVC/ZnO nanocomposite and PVC membranes

The zeta potential results of the PVC/ZnO nanocomposite and PVC membranes are presented in Fig. 7. Both PVC/ZnO nanocomposite and PVC membranes exhibited negative charges. However, it was worth noting that the PVC membrane isoelectric point becomes nearby pH = 7.8. Zeta potential of the composite back surface was analyzed at pH = 7.8 after etching off the PVC support membrane to examine the charge properties of the interlayer between the PVC substrate and the outermost surface.

The zeta potential of the PVC membrane was increasing with pH decreasing because of the addition of hydrogen ions from HCl and decreasing by the increasing of pH because of the presence of OH^- ions from NaOH. The zeta potential of PVC/ZnO nanocomposite and PVC membranes were negative charges throughout the 4–11 and 8.5–11 pH range, respectively. Hence, it was predicted that the zeta potential of the original membrane (PVC membrane) would be lower compared to the membrane modified with ZnO NPs. The point of zero charges for PVC membrane was reached at pH 8, unlike in PVC membrane where the surface remained negative. The implicit explanation was that the PVC membrane would transfer a negative surface on the membrane over a wide range of pH (4–11) while ZnO NPs would remain mostly positive in neutral to acidic conditions.

3.2. Effect of ZnO NPs ratios

Fig. 8 shows the effect of ZnO NPs ratio on the degradation of basic brown 1 dye. Experiments were performed for 6 h with different ratios of ZnO NPs (0.1%–3%) to determine the rate of dye degradation. The initial dye concentration was 20 mg/L. Fig. 8 shows that, when using ratios ranging from 0.1% to 3% of ZnO NPsas a filler to the prepared nanocomposite membrane, the removal and chemical adsorption of the basic brown 1 dye on the surface of the nanocomposite membrane increases up to 93% at 3% of ZnO NPs. It was concluded that increasing

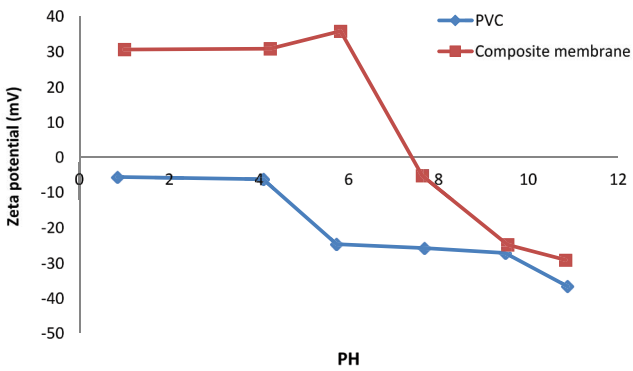

Fig. 7. Effect of pH on zeta potential for PVC/ZnO nanocomposite and PVC membranes.

the percentage of zinc oxide increases the positive charge of the prepared nanocomposite membrane, which maximizes the removal process of basic brown 1 dye.

But there is a slight increase in *R*% due to the release of intermediate oxidation products from ZnO NPs. As these intermediate products are considered more hydrophilic as a result of the oxidation reaction, they are not strongly absorbed on the surface of ZnO NPs, and thus dissolve again in the bulk water. The subsequent increase in the measured *R*% was attributed to the mineralization of the intermediate products due to catalytic oxidation. However, the dye removal %*R* of 1% ZnO NPs reached the same plateau value as in the higher ZnO NPs experiments, indicating that only the kinetics were slower for the dilute ZnO NPs, but the extent of oxidation and removal was similar.

3.3. Effect of solution pH

Dye decolorization destruction of carbon skeleton was studied through pH change (3–11) using NaOH and H_2SO_4 0.1 M solutions to adjust the dye solution's pH. Basic brown 1 dye concentration and PVC/ZnO nanocomposite membrane that was used for the removal process at room temperature were 500 mg/L and 0.5 g/L, respectively. As shown in Fig. 9, increase the pH of the solution from pH 3 to 5, the decolorization of basic brown 1 dye was increased. The maximum degradation was achieved at pH 7 and decrease at alkaline medium due to dissolution of ZnO NPs in the dye solution. PVC/ZnO nanocomposite membrane gives complex as $[Zn(OH)_4]^{2-}$ at pH > 7 forms while at pH < 7, the corresponding salt was produced. PVC/ZnO nanocomposite membrane shows low reactivity because of the dissolution of ZnO of PVC/ZnO nanocomposite membrane in acidic and basic pH, respectively [28–31]. It was found that the maximum dye removal of 93.6% was recorded at the pH ~4.5.

3.4. Effect of basic brown 1 dye concentrations

The effect of basic brown 1 dye concentrations on the degradation of dye was evaluated by varying the dye concentrations from 10 to 1,000 mg/L with the prepared PVC/ZnO nanocomposite membrane at constant pH ~4.5 (Fig. 10). It is clear from the figure, as the initial dye concentration increases, the degradation of basic brown 1 dye increases. This relates to the information of –OH radicals reacting with basic brown 1 dye molecules. As the active sites were covered with the dye ions, the generation of OH radicals on the surface of the membrane was enhanced, and also the path length of the photons entering the dye solution increases. The results clearly demonstrated that the PVC/ZnO nanocomposite membrane adsorption filtration process was efficient at a low concentration of dye.

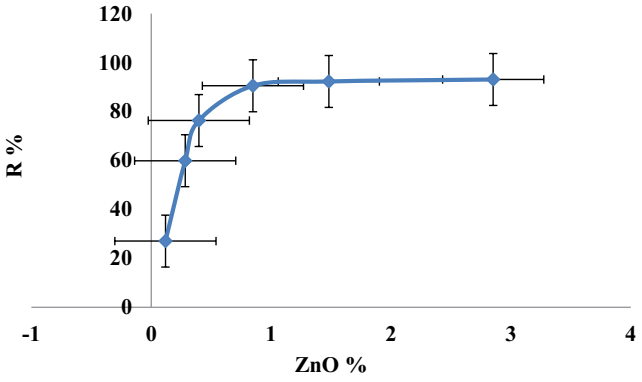

Fig. 8. Effect of ZnO NPs ratio on the degradation of basic brown 1 dye (conditions: basic brown 1 dye = 20 mg/L; UV intensity = 3.4 mW/cm^2; initial pH 7.5).

3.5. Effect of time

Immerse the prepared membrane in a test tube containing (100 mg/L) the dye solution and kept stature without shaking for 70 min. It was observed that after 60 min, the solution became clear as the dye was adsorbed. Notice that the concentration of basic brown 1 dye was varied from the bottom than the above solution. This well-indicates the ability of the membrane to binding with dyes, where the dye removal efficiency by ZnO/PVC nanocomposite membrane reached 98.6% in 60 min (Fig. 11). No doubt that the membrane is a good adsorbent potential for the removal of dyes from water solution due to its unique chemical composition.

3.6. Adsorption kinetics

The kinetics of adsorption basic brown 1 dye adsorbed on PVC/ZnO nanocomposite membrane were evaluated to

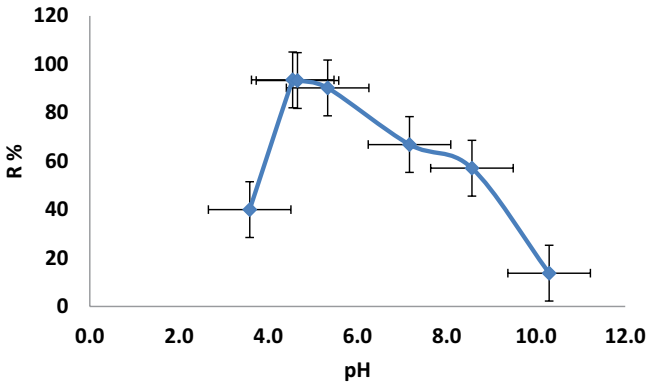

Fig. 9. Effect of pH on the rejection of basic brown 1 dye using PVC/ZnO nanocomposite membrane.

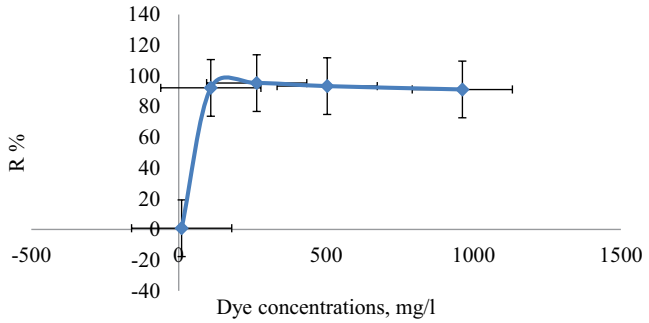

Fig. 10. Effect of basic brown 1 dye concentrations, mg/L (pH ~4.5, *p* = 5 bar).

explain the adsorption mechanism via kinetics models of the pseudo-first-order and pseudo-second-order as shown in Figs. 12a and b, respectively.

Table 1 shows the pseudo-second-order correlation coefficients (R^2) of basic brown 1 dye (0.99) were higher than the R^2 of pseudo-first-order correlation coefficient (0.97). These values confirm that the kinetic pseudo-second-order model was suitable for the adsorption kinetics of basic brown 1 dye onto PVC/ZnO nanocomposite membrane. This means that the rate-limiting step of the process may be the chemical adsorption process.

3.7. Adsorption isotherms

The results obtained from adsorption isotherms for basic brown 1 dye by PVC/ZnO nanocomposite membrane are shown in Figs. 13a and b.

According to the results in Table 2, a higher value of R^2 (0.99) indicated that adsorption of basic brown 1 dye by PVC/ZnO nanocomposite membrane was well-performed by Langmuir isotherm. In addition to the Langmuir constant ($0 < R_1 < 1$), the tested dyes' values and representing a favorable adsorption process by the nanocomposite membrane. This explained that the adsorption was taking place on homogeneous sites as a monolayer process.

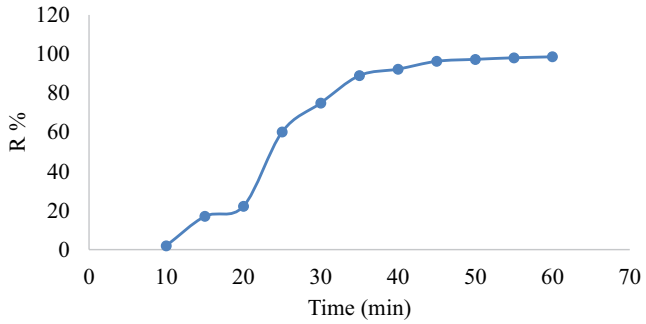

Fig. 11. Effect of time on the PVC/ZnO nanocomposite membrane for basic brown 1 dye adsorption.

3.8. Mechanism of nanocomposite membrane adsorption

From the results of isothermal, adsorption kinetics, and zeta optional, it can be considered that the adsorption of the basic brown 1 dye was a chemical reaction between cationic dyes and ZnO NPs for nanofilm-based adsorbers. However, electrostatic repulsion between the cationic dyes and the positive charges on ZnO NPs led to increase the pH of the dyes, at a higher basic pH, and lower positively charged sites and negatively charged sites were settled on the ZnO NPs surface, which would prefer cationic dye adsorption as the electrostatic attractions. The formation of OH ions at the same time leads to a contest between the OH ions and the cationic dye to inhabit nanoparticles adsorption sites, consequently favor the adsorption of cationic dyes.

Due to the presence of oxygen defect states, ZnO Nps in the composite membrane ZnO NPs can improve the tiny

Table 1
Parameters of adsorption kinetics of basic brown 1 dye onto PVC/ZnO nanocomposite membrane

Model	Parameters	Value
Pseudo-first-order	R^2	0.779999
	k_1 (min^{-1})	0.04063
	q_e (mg/g)	12.53173
Pseudo-second-order	R^2	0.990001
	k_2 (g mg^{-1} min^{-1})	0.14759
	q_e (mg/g)	72.56613

Table 2
Adsorption isotherm parameters for the adsorption of basic brown 1 dye onto the PVC/ZnO nanocomposite membrane

Dye	Langmuir isotherm			Freundlich isotherm	
	q_m (mg/g)	R_L	R^2	n	R^2
Basic brown 1	100.20	0.87	0.99	1.02	0.97

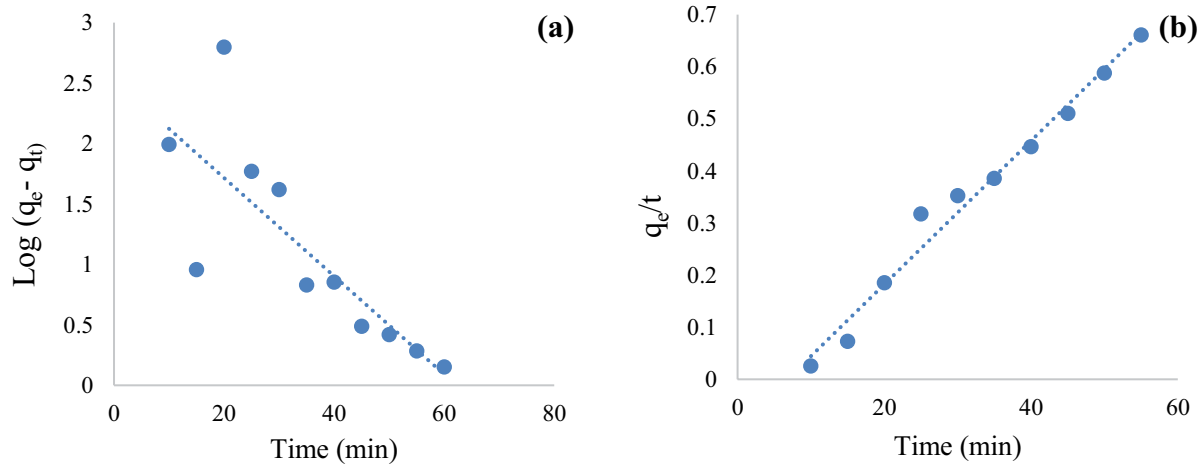

Fig. 12. Adsorption kinetic models for basic brown 1 dye onto PVC/ZnO nanocomposite membrane: (a) pseudo-first-order and (b) pseudo-second-order.

charge separation. Apart from this, defect states in the ZnO Nps provide the narrowing in the bandgap which further facilitates the electron transfer from the dye to ZnO Nps. Under high dye accumulations, electron–hole pair creates in their respective conduction band and valance band of ZnO NPs. Heterojunction creation among ZnO and dye generates the synergetic effect. The enhanced electrons concentration in the conduction band of ZnO increases the basic brown 1 dye degradation process by generating the reactive superoxide (O^{2-}) radicals from surface oxygen molecules. Similarly, the enhanced holes concentration in the valance band of basic brown 1 dye transforms the water molecule into hydroxyl radicals (•OH). These two unsaturated radicals hydroxyl radicals and superoxide radicals destroy the organic dye molecules [40,41]. The charge transfer mechanism for composite membrane decorated ZnO Nps is schematically presented in Fig. 14.

The extremely enhanced adsorption–degradation activity of PVC composite membrane modified ZnO Nps, was optimized and achieved through the surface modification using ZnO Nps NPs [42,43]. Also, the retardation in the adsorption–degradation activity appears due to the reduction in the effective surface area of PVC composite membrane and enhancement in the defect concentration in ZnO Nps.

4. Conclusion

The process of adsorption–ultrafiltration has been successfully applied for basic brown 1 dye removal from synthetic wastewater solutions using the prepared PVC/ZnO nanocomposite membrane. PVC was used as an ultrafiltration membrane, while ZnO NPs were used as a catalyst. The PVC was characterized by high chemical stability and high physical strength to withstand high pressures during

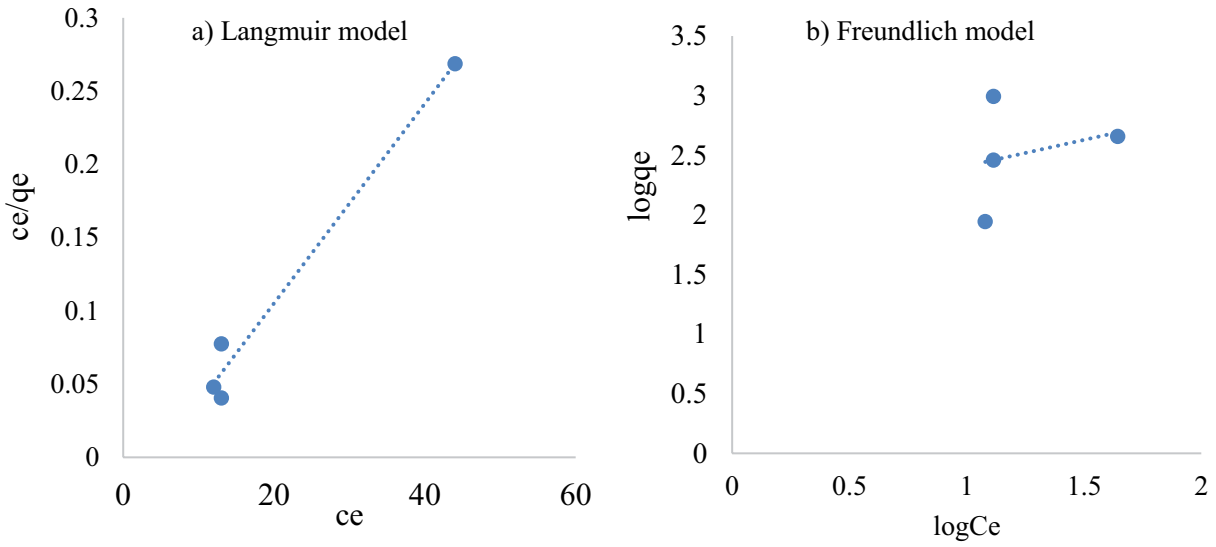

Fig. 13. Adsorption isotherm parameters for the adsorption of basic brown 1 onto the PVC/ZnO nanocomposite membrane.

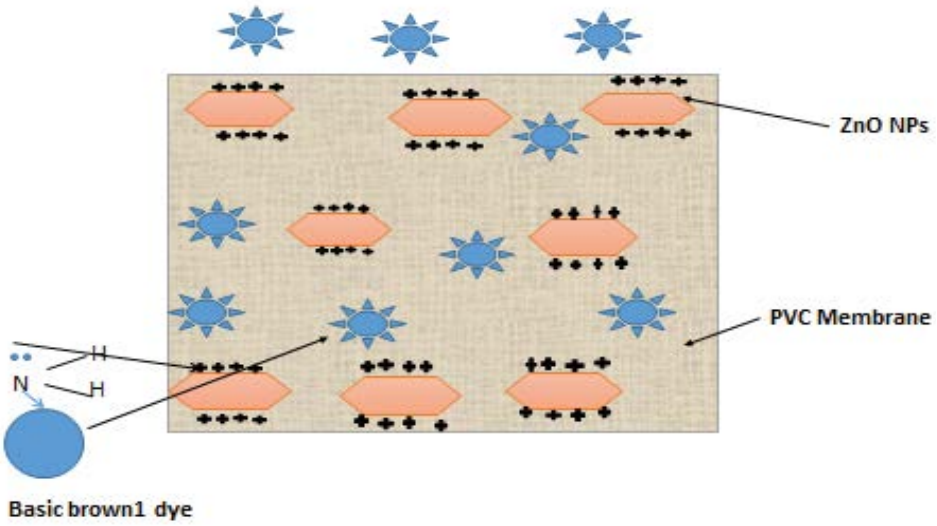

Fig. 14. Mechanism of dye adsorption process on the PVC/ZnO nanocomposite membrane.

the desalination or water treatment process, and ZnO NPs were of a high adsorption capacity of dyes and decomposition of dyes due to its positive charge that increasing the chemical adsorption strength. Consequently, the prepared PVC/ZnO nanocomposite membrane possess dual function "adsorption and filtration processes". The adsorption and filtration processes were dependent on the pH that evidence, where the dye rejection was more efficient at acidic conditions than at "neutral and alkaline" at pH 4.5 the dye rejection efficiency values was 98.6% from synthetic water after 60 min. From the kinetics and isotherm studies of adsorption basic brown 1 dye adsorbed on PVC/ZnO nanocomposite membrane, pseudo-second-order model and Langmuir were suitable for the adsorption kinetics and isotherm. Consequently, it was assumed that the rate-limiting step may be the chemical adsorption process and the adsorption was taking place on homogeneous sites as a monolayer process. Finally, the treatment process is characterized by low-energy requirements included in the adsorption-ultrafiltration process "it can be operated without heating", the very fast reaction kinetics, and the high selectivity for the basic brown 1 dye removal. Also, the membrane is low expensive, improving performance, and extending life expectancy.

References

[1] A.A. Emam, M. Fathy, R. Hosny, A.S. Naeim, Surface modification of TiO_2@Pvc composite membrane for textile dye house (Brome Phenol Blue) filtration, Pet. Chem. Ind. Int., 3 (2020) 10–14.

[2] A. Hasanbeigi, Energy-Efficiency Improvement Opportunities for the Textile Industry, Lawrence Berkeley National Lab. (LBNL), Berkeley, CA, 2010.

[3] D.P. Loucks, E. Van Beek, Water Resource Systems Planning and Management: An Introduction to Methods, Models, and Applications, Springer, Cham, 2017.

[4] J. Mittal, Permissible synthetic food dyes in India, J. Sci. Educ., 25 (2020) 567–577.

[5] S. Wong, N.A.N. Yac'cob, N. Ngadi, O. Hassan, I.M. Inuwa, From pollutant to solution of wastewater pollution: synthesis of activated carbon from textile sludge for dye adsorption, Chin. J. Chem. Eng., 26 (2018) 870–878.

[6] I. Anastopoulos, I. Pashalidis, A.G. Orfanos, I.D. Manariotis, T. Tatarchuk, L. Sellaouid, A. Bonilla-Petriciolete, A. Mittal, A. Núñez-Delgado, Removal of caffeine, nicotine and amoxicillin from (waste) waters by various adsorbents. A review, J. Environ. Manage., 261 (2020) 110236, doi: 10.1016/j.jenvman.2020.110236.

[7] S. Soni, P.K. Bajpai, J. Mittal, C. Arora, Utilisation of cobalt doped iron based MOF for enhanced removal and recovery of methylene blue dye from wastewater, J. Mol. Liq., 314 (2020) 113642, doi: 10.1016/j.molliq.2020.113642.

[8] C. Arora, S. Soni, S. Sahu, J. Mittal, P. Kumar, P.K. Bajpai, Iron based metal organic framework for efficient removal of methylene blue dye from industrial waste, J. Mol. Liq., 284 (2019) 343–352.

[9] I. Anastopoulos, A. Mittal, M. Usman, J. Mittal, G. Yu, A. Núñez-Delgado, M. Kornaros, A review on halloysite-based adsorbents to remove pollutants in water and wastewater, J. Mol. Liq., 269 (2018) 855–868.

[10] A. Mittal, J. Mittal, Chapter 11 – Hen Feather: A Remarkable Adsorbent for Dye Removal, S.K. Sharma, Ed., Green Chemistry for Dyes Removal from Wastewater, Scrivener Publishing LLC, USA, 2015, pp. 409–457.

[11] G.T. Güyer, K. Nadeem, N. Dizge, Recycling of pad-batch washing textile wastewater through advanced oxidation processes and its reusability assessment for Turkish textile industry, J. Cleaner Prod., 139 (2016) 488–494.

[12] M. Keshawy, M. Fathy, A. Gaafar, R. Hosny, T. Abd Elmoghny, Low-cost bio-adsorbent based on amorphous carbon thin film/chitosan composite for removal of methylene blue dye from aqueous solutions: kinetic and isotherm, Egypt. J. Chem., 62 (2019) 2313–2329.

[13] C. Yu, X. Huang, H. Chen, H.C.J. Godfray, J.S. Wright, J.W. Hall, P. Gong, S. Ni, S. Qiao, G. Huang, Managing nitrogen to restore water quality in China, Nature, 567 (2019) 516–520.

[14] M. Qadir, B.R. Sharma, A. Bruggeman, R. Choukr-Allah, F. Karajeh, Non-conventional water resources and opportunities for water augmentation to achieve food security in water scarce countries, Agric. Water Manage., 87 (2007) 2–22.

[15] M. Salgot, M. Folch, Wastewater treatment and water reuse, Curr. Opin. Environ. Sci. Health, 2 (2018) 64–74.

[16] N.R. Council, Water Reuse: Potential for Expanding the Nation's Water Supply Through Reuse of Municipal Wastewater, National Academies Press, Washington, DC, 2012.

[17] R. Hosny, M. Fathy, O.H. Abd Elraheem, M.A. Zayed, Utilization of cross-linked chitosan/ACTF biocomposite for softening hard water: optimization by adsorption modeling, Egypt. J. Chem., 62 (2019) 437–456.

[18] A.F.M. Udaiyappan, H.A. Hasan, M.S. Takriff, S.R.S. Abdullah, A review of the potentials, challenges and current status of microalgae biomass applications in industrial wastewater treatment, J. Water Process Eng., 20 (2017) 8–21.

[19] A. Deegan, B. Shaik, K. Nolan, K. Urell, M. Oelgemöller, J. Tobin, A. Morrissey, Treatment options for wastewater effluents from pharmaceutical companies, Int. J. Environ. Sci. Technol., 8 (2011) 649–666.

[20] P. Krzeminski, M.C. Tomei, P. Karaolia, A. Langenhoff, C.M.R. Almeida, E. Felis, F. Gritten, H.R. Andersen, T. Fernandes, C.M. Manaia, Performance of secondary wastewater treatment methods for the removal of contaminants of emerging concern implicated in crop uptake and antibiotic resistance spread: a review, Sci. Total Environ., 648 (2019) 1052–1081.

[21] B. Van der Bruggen, Ç.B. Canbolat, J. Lin, P. Luis, The Potential of Membrane Technology for Treatment of Textile Wastewater, A. Figoli, A. Criscuoli, Eds., Sustainable Membrane Technology for Water and Wastewater Treatment, Springer, Singapore, 2017, pp. 349–380.

[22] C.A. López-Morales, L. Rodríguez-Tapia, On the economic analysis of wastewater treatment and reuse for designing strategies for water sustainability: lessons from the Mexico Valley Basin, Resour. Conserv. Recycl., 140 (2019) 1–12.

[23] K. Senthilkumar, A. Mollier, M. Delmas, S. Pellerin, T. Nesme, Phosphorus recovery and recycling from waste: an appraisal based on a French case study, Resour. Conserv. Recycl., 87 (2014) 97–108.

[24] A. Ahmad, S.H. Mohd-Setapar, C.S. Chuong, A. Khatoon, W.A. Wani, R. Kumar, M. Rafatullah, Recent advances in new generation dye removal technologies: novel search for approaches to reprocess wastewater, RSC Adv., 5 (2015) 30801–30818.

[25] M.F. Tay, C. Liu, E.R. Cornelissen, B. Wu, T.H. Chong, The feasibility of nanofiltration membrane bioreactor (NF-MBR)+ reverse osmosis (RO) process for water reclamation: comparison with ultrafiltration membrane bioreactor (UF-MBR)+ RO process, Water Res., 129 (2018) 180–189.

[26] I. Petrinic, J. Korenak, D. Povodnik, C. Hélix-Nielsen, A feasibility study of ultrafiltration/reverse osmosis (UF/RO)-based wastewater treatment and reuse in the metal finishing industry, J. Cleaner Prod., 101 (2015) 292–300.

[27] K. Wieszczycka, K. Staszak, Polymers in separation processes, Phys. Sci. Rev., 2 (2017) 32.

[28] Z. Yang, Y. Zhou, Z. Feng, X. Rui, T. Zhang, Z. Zhang, A review on reverse osmosis and nanofiltration membranes for water purification, Polymers, 11 (2019) 1252, doi: 10.3390%2Fpolym11081252.

[29] O.D. Ojajuni, Removal of Organic Micropollutants in Water Using Surface Modified Membrane Systems, University of Surrey, 2017.

[30] M. Barakat, E. Schmidt, Polymer-enhanced ultrafiltration process for heavy metals removal from industrial wastewater, Desalination, 256 (2010) 90–93.

[31] K.N. Jacob, S.S. Kumar, A. Thanigaivelan, M. Tarun, D. Mohan, Sulfonated polyethersulfone-based membranes for metal ion removal via a hybrid process, J. Mater. Sci., 49 (2014) 114–122.
[32] J. Hasnidawani, H. Azlina, H. Norita, N. Bonnia, S. Ratim, E. Ali, Synthesis of ZnO nanostructures using sol–gel method, Procedia Chem., 19 (2016) 211–216.
[33] R. Singh, K.K. Mohanty, Foams stabilized by *in-situ* surface-activated nanoparticles in bulk and porous media, Soc. Pet. Eng. J., 21 (2016) 121–130.
[34] D.N. Yadav, K.A. Kishore, B. Bethi, S.H. Sonawane, D. Bhagawan, ZnO nanophotocatalysts coupled with ceramic membrane method for treatment of Rhodamine-B dye wastewater, Environ. Dev. Sustainability, 20 (2018) 2065–2078.
[35] I.M. Banat, P. Nigam, D. Singh, R. Marchant, Microbial decolorization of textile-dyecontaining effluents: a review, Bioresour. Technol., 58 (1996) 217–227.
[36] C. Namasivayam, M.D. Kumar, K. Selvi, R.A. Begum, T. Vanathi, R. Yamuna, 'Waste'coir pith—a potential biomass for the treatment of dyeing wastewaters, Biomass Bioenergy, 21 (2001) 477–483.
[37] E. Evgenidou, K. Fytianos, I. Poulios, Semiconductor-sensitized photodegradation of dichlorvos in water using TiO_2 and ZnO as catalysts, Appl. Catal., B, 59 (2005) 81–89.
[38] A. Gouthaman, A. Gnanaprakasam, V. Sivakumar, M. Thirumarimurugan, M.A.R. Ahamed, R. Azarudeen, Enhanced dye removal using polymeric nanocomposite through incorporation of Ag doped ZnO nanoparticles: synthesis and characterization, J. Hazard. Mater., 373 (2019) 493–503.
[39] M. Landarani, M.A. Chamjangali, B. Bahramian, Preparation and characterization of a novel chemically modified PVC adsorbent for methyl orange removal: optimization, and study of isotherm, kinetics, and thermodynamics of adsorption process, Water Air Soil Pollut., 231 (2020) 1–17.
[40] M. Fathy, H.R. Ali, Y.M. Moustafa, A. El Shahawy, Removal of suspended matter and salts on ultrafiltration cellulose acetate/expanded polystyrene waste grafted PEG composite membrane, Desal. Water Treat., 197 (2020) 30–40.
[41] M. Fathy, A. El Shahawy, T. Moghny, A. Nafady, Enhanced desalination process using a Cu–ZnO-polyvinyl chloride-nylon nanofiltration membrane as a calcite antiscalant in reverse osmosis, Mater. Express, 10 (2020) 671–679.
[42] H. Hassan, M.S. Ahmed, M. Fathy, M.S. Yousef, Impact of salty water medium and condenser on the performance of single acting solar still incorporated with parabolic trough collector, Desalination, 480 (2020) 114324, doi: 10.1016/j.desal.2020.114324.
[43] A.M. Zayed, M. Fathy, M. Sillanpää, M.S.M.A. Wahed, Talc-graphite schist as a natural organo-mineral complex for methylene blue remediation: kinetic and isotherm study, SN Appl. Sci., 2 (2020) 1–17.